Heat and contaminant transport in unsaturated soil

Hasan Ghasemzadeh
Khajeh-Nasiral'din Toosi University of Technology, Tehran, Iran

Abstract: *Solute transport in unsaturated porous media can be viewed as a coupled phenomenon with water and heat transport, together with mechanical behaviour of media. In this paper, solute transport is formulated mathematically considering heat and water flow in deformable porous media. Advection, dispersion and diffusion of chemical species in the liquid phase are considered. Convection and conduction for heat flow is taken into account. Water flow is considered in both vapour and liquid phases. Equilibrium equation, energy conservation, mass conservation and linear momentum for water, gas and solute are written and solved simultaneously using finite element method. The developed model is validated by solving some examples and comparing results with the results of experimental observation.*

Introduction

Transfer of contaminant in soil is an issue of great importance with respect to the associated risks to human health and the environment. The advection–dispersion equation (ADE) has been widely used to describe solute transport in porous media (Bear, 1979; Fetter, 1993). In spite of numerous studies of contaminant transport in saturated porous media, few researches are accessible in unsaturated porous media especially in case of existing thermal forces (e.g. Schrefler, 1995 ; Gens and Olivella, 2000, 2001 and Thomas et al., 2004).

Transfer of contaminant in soil is a problem with coupling between different forces. Variations of pressure and temperature induce water velocity changes and contaminant transport. Also, in some clayey soils, osmotic pressure is another force in water and solute transport. In a number of environmental geomechanics situations, problems often involve heat, mass and contaminant transport simultaneously and coupling solution is needed. This paper gives the governing equations of the thermal, chemical and mechanical behaviour in order to estimate deformation, temperature and concentration of chemical elements in a multiphase medium.

Most of the present studies are a combination between one thermo-hydro-mechanical program and one geochemical program. Using the two existing codes is the major advantage of this method, although it is the origin of some inconveniences too. The governing equations are solved in two programs in this method in which some variables are kept constant in each program. Using one iterative method to find the exact value of all variables requires spending a lot of time to solve and may cause inaccuracy in results. In addition, it is necessary to develop proper hydro- mechanical constitutive models that take into account the influence of geochemical variables on soil behaviour (Gens et al. 2002). Herein the chemical transport equation is combined with thermo-hydro-mechanical equations in a fully coupled manner and the equations are solved simultaneously with finite element method.

Based on the theory of Philip & De Vries (1957) for transfer of heat and humidity in rigid medium, Gatmiri et al. (1999) have proposed and validated a coupled formulation for behaviour of a deformable unsaturated porous medium. In this approach, water flow occurs in both vapour and liquid phases; and heat convection and conduction have been taken into account. The coupling effects of skeleton, suction and temperature via the concept of state surface of void ratio and degree of saturation have been included. In this paper to include the chemical transfer in the unsaturated soil, advection, dispersion and diffusion of contaminant are considered. The interaction of chemical solute on the mechanical behaviour is considered via void ratio surface. The governing equations in terms of soil displacements, water and air pressure, temperature and concentration of contaminant are coupled. The results of this coupling are non-linear partial differential equations which are

solved by finite element method.

Governing equations

Mass conservation of moisture, gas and chemical species as well as energy conservation and equilibrium equation are the governing equations of this formulation which are explained as follows:

Gas mass conservation

Darcy's law can be used to determine gas velocity in porous media (Matyas, 1967; Langfelder et al., 1968), therefore:

$$V_g = -K_g\left(\nabla\left(\frac{P_g}{\gamma_g}\right)+\nabla Z\right) \quad (1)$$

where K_g and P_g are the permeability and the pressure of gas in the porous media respectively. Gas permeability is a function of the void ratio and the degree of saturation (Lloret and Alonso, 1980 ; Thomas and He, 1995) and can be written as:

$$K_g = \frac{b\gamma_g}{\mu_g}\left[e(1-S_r)\right]^c \quad (2)$$

where e is the void ratio, S_r is the degree of saturation, b and c are constant determined experimentally and μ_g, γ_g are the viscosity and the unit weight of gas, respectively.

Considering flux of dissolved gas in the water, equation of mass conservation and movement of gas in a control volume of unsaturated porous media can be given as:

$$\frac{\partial}{\partial t}\left[n\rho_g\left(1-S_r+\mathrm{H}S_r\right)\right] = -div\left(\rho_g V_g\right)-div\left(\rho_g \mathrm{HU}\right) \quad (3)$$

where H is Henry constant, n porosity, ρ_g gas density and V_g, U are vectors of gas and water velocity, respectively.

Moisture mass conservation

Moisture stands for water and vapour in this formulation. Moisture mass conservation is as follow:

$$\frac{\partial \rho_m}{\partial t} = -div\left(\rho_w(\mathbf{U}+\mathbf{V})\right) \quad (4)$$

where U and V are water and vapour velocity, ρ_w is water density and ρ_m is moisture density which is equal to:

$$\rho_m = \theta\rho_w + (n-\theta)\rho_v = nS_r\rho_w + n(1-S_r)\rho_v \quad (5)$$

where ρ_v is the vapour density and θ is the volumetric water content.

Generalized Darcy's law has been proposed for water transport in unsaturated soil by many authors (e.g. Richards, 1931; Bear, 1979). Using this law, the velocity of water (U) would be:

$$\mathbf{U} = -K_w\nabla(P) \quad (6)$$

where Kw is permeability of water. In addition to capillary and gravitational potential, osmotic potential may change water velocity where there is solute in some types of soils (Mitchell, 1993). To consider the osmotic pressure, can be written as:

$$\nabla(P) = \nabla(\Psi_m + Z) + \omega\nabla(\Psi_o) \quad (7)$$

where Ψ_m is the capillary potential, Ψ_0 osmotic potential, Z gravitation term and, ω is the osmotic efficiency. Value of osmotic efficiency depends on the soil and the solute properties and has been measured for many types of clay (Bresler, 1973; Barbour and Fredlund, 1989). In this formulation, we assume that the osmotic efficiency is an exponential function of the water content and the concentration of solute, then

$$\omega = \omega(C,\theta) = \alpha\exp(\beta\theta+\gamma C) \quad (8)$$

where C is the solute concentration and α, β, γ are the parameters that should be determined for each solute and soil system. Osmotic efficiency has a value between 0 and 1.

For dilute solution, osmotic potential (Ψ_0) can be obtained from Van't Hoff equation:

$$\Psi_o = -\frac{RTC}{\gamma_w} \quad (9)$$

where T is the temperature in Kelvin and R is the universal gas constant (R =8.314 J/mol/°K).

Capillary potential (Ψ_m) can be replaced with:

$$\Psi_m = \frac{\sigma(T)}{\sigma_r}\Psi_r(\theta) \tag{10}$$

where $\sigma(T)$ is the surface tension of water at temperature T. Ψ_r and σ_r are the capillary potential and the surface tension in reference temperature (r). Substituting equations (7) to (10) into equation (6), the velocity of water in unsaturated media is obtained as follows:

$$\mathbf{U} = -K_w \nabla(P) = -D_{Twc}\nabla T - D_{\theta w}\nabla\theta - D_{cw}\nabla C + K_w \nabla Z \tag{11}$$

where

$$D_{Twc} = K_w \frac{\Psi_r(\theta)}{\sigma_r}\frac{d\sigma(T)}{dT} + K_w \frac{RC}{\gamma_w}\omega(\theta, C) \tag{12}$$

$$D_{\theta w} = K_w \frac{\sigma(T)}{\sigma_r}\frac{d\Psi_r}{d\theta} \tag{13}$$

$$D_{cw} = K_w \frac{RT}{\gamma_w}\omega(\theta, C) \tag{14}$$

in which K_w is the permeability of water in the porous media. In unsaturated porous media, the general form of permeability is:

$$K_w = K_{rw}(S_r).K(n)/\mu_w \tag{15}$$

where $K_{rw}(S_r)$ is the relative permeability that depends on the degree of saturation, $K(n)$ is the intrinsic permeability that depends on the porosity and μ_w is the water viscosity that depends on the temperature. Different relations for permeability have been proposed by various investigators (Irmay, 1954 ; Corey, 1957 ; Gardner, 1958 ; Kovacs, 1981 ; Gens et al., 1997) which can be classified in the above form. In this study, the following relationship has been adopted (Gatmiri, 1997):

$$K_{\mathrm{w}} = K_{\mathrm{wz0}}\left(\frac{S_r - S_{ru}}{[1 - S_{ru}]}\right)^d \left(\frac{\mu_{\mathrm{w}}(T_{\mathrm{r}})}{\mu_{\mathrm{w}}(T)}\right) \tag{16}$$

where $K_{wz0}=c_1.10^{c_2 e}$ saturated soil water permeability, $\mu_w(T_r)$, $\mu_w(T)$ are the water viscosity at reference temperature (T_r) and at temperature(T). e and S_{ru} are the void ratio and the residual degree of saturation, respectively and c_1, c_2 and d are constant.

Flux of vapour (q_{vap}) is (Philip & De Vries 1957):

$$q_{vap} = -D_0.\nu.\tau.a.\nabla\rho_v \tag{17}$$

where D_0 is the molecular diffusion of vapour, τ tortuosity, a air content of soil and ν is the constant which is approximately equal 1.0 in the ambient condition. The vapour density (ρ_v) in the thermodynamic equilibrium condition is a function of the saturation vapour density (ρ_0) and the humidity (h):

$$\rho_v = \rho_0 h \tag{18}$$

The saturation vapour density (ρ_0) is temperature dependent and the humidity can be expressed by Kelvin relation:

$$h = \exp\left(\frac{\Psi g}{R_f T}\right) \tag{19}$$

Where Ψ is the thermodynamic potential, g is the gravity, R_f is the fluid constant and T is the temperature.

In the ambient condition, variation of relative humidity against temperature can be neglected (Philip & De Vries,1957; Farouki, 1986) and it can be assumed that relative humidity is a function of water content. Substituting equations (18), (19) in equation (17), we can obtain the vapour velocity (V) as:

$$\mathbf{V} = \frac{q_{vap}}{\rho_w} = -\frac{D_0.\nu.\tau.a}{\rho_w}.\frac{\rho_v g}{RT}\frac{\partial\psi}{\partial\theta}\nabla\theta - \frac{D_0.\nu.\tau.a}{\rho_w}\frac{d\rho_0}{dT}h\nabla T \tag{20}$$

Chemical species transport and conservation

Chemical species move in porous media through convection and diffusion phenomena. Convective flow (q_c) or transfer of solute due to water flow is:

$$q_c = \mathrm{U}C \tag{21}$$

where U is the water velocity and C is the solute concentration. Diffusive and dispersive flow of solute is likewise proportional to the gradient of concentration (Ficks law):

$$q_{diff} = -\mathbf{D}grad(C) \tag{22}$$

where D is the hydrodynamics dispersion tensor that is sum of the effective diffusion tensor and the mechanical dispersion tensor:

$$\mathbf{D} = D_{diff} + D_{disp} \tag{23}$$

where D_{diff} is the molecular diffusion tensor and D_{disp} is the mechanical dispersion tensor of porous media. Scheidegger (1961) stated that the coefficients of mechanical dispersion can be related to the average interstitial fluid velocity by means of the geometric dispersivity of the medium. For a saturated porous medium, the geometric dispersivity depends on the hydraulic conductivity, the length of a characteristic flow path, and the tortuosity. In a medium that is isotropic with respect to dispersion, the geometric dispersivity can be expressed in terms of just two coefficients: longitudinal dispersivity and transverse dispersivity (Bear, 1979). In the two dimension problems it takes the following form:

$$D_{xx} = \alpha_L \frac{v_x^2}{|v|} + \alpha_T \frac{v_y^2}{|v|} \tag{24}$$

$$D_{yy} = \alpha_L \frac{v_y^2}{|v|} + \alpha_T \frac{v_x^2}{|v|} \tag{25}$$

$$D_{xy} = D_{yx} = (\alpha_L - \alpha_T)\frac{v_x v_y}{|v|} \tag{26}$$

where v_x, v_y are the velocity of water in x and y direction and v is the mean velocity of water.

Mass conservation of chemical species without any interaction with solid phase can be expressed as:

$$\frac{\partial(\theta C)}{\partial t} = -\mathrm{div}((1-\omega)(q_{diff} + q_c)) + \Sigma R_n \tag{27}$$

Energy conservation and heat flow

In porous medium, the energy conservation can be written as:

$$\frac{\partial \varphi}{\partial t} + \mathrm{div}Q = 0 \tag{28}$$

where Q is the heat flow and φ is the volumetric bulk heat content of medium which can be defined by :

$$\varphi = C_T(T - T_0) + (n - \theta)\rho_v h_{fg} \tag{29}$$

in which h_{fg} is the latent heat of vaporization and C_T is the specific heat capacity of unsaturated mixture and can be written as:

$$C_T = (1-n)\rho_s C_{ps} + \theta\rho_w C_{pw} + (n-\theta)\rho_v C_{pv} + (n-\theta)\rho_g C_{pg} + \theta C M_c C_{pc} \tag{30}$$

where M_c is the molar mass of solute and C_{ps}, C_{pw} , C_{pv}, C_{pg} and , C_{pc} are the specific heat capacity of solid, liquid, vapour, gas and solute, respectively. Total flow of latent and sensible heat in an unsaturated porous medium is given, based on Philip & De Vries theory as:

$$Q = -\lambda grad T + \left[C_{Pw}\rho_w U + C_{pv}\rho_w V + C_{pg}\rho_g V_g + C_{Pc}(q_c + q_{diff})\right](T - T_0) + \rho_w h_{fg} V + \rho_v V_g h_{fg} \tag{31}$$

where T_0 is an arbitrary reference temperature and λ accounts for Fourier heat diffusion coefficient and can be evaluated by following proposition :

$$\lambda = (1-n)\lambda_s + \theta\lambda_w + (n-\theta)\lambda_v \tag{32}$$

in which λ_s, λ_w and λ_v are the thermal conductivity of soil, water and vapour.

Equilibrium equation and constitutive law

Equilibrium equation, for unsaturated media using total stress can be written as:

$$(\sigma_{ij} - \delta_{ij} p_g)_{,j} + p_{g,j} + b_i = 0 \tag{33}$$

where σ is the stress tensor, pg pressure of gas, δ_{ij} Kronecker delta and b_i is the volumetric force in direction i.

Stress variables governing unsaturated soil behaviour can be reduced to two stress state variables. Net stress and suction are considered as two independent stresses in present study. Nonlinear elastic behaviour against mechanical,

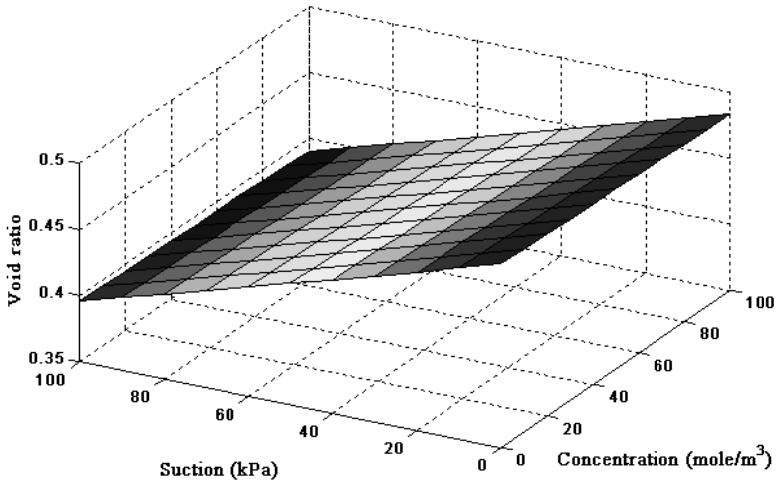

Fig. 1 Void ratio surface (the mean stress and the temperature are constant: T=20°C, σ=30kPa)

thermal and chemical forces is assumed. For this condition the constitutive law can be written as:

$$d(\sigma_{ij} - \delta_{ij}p_g) = Dd\varepsilon - Fd(p_g - p_w) - C_T dT - L_C dC \tag{34}$$

where

$F = DD_s^{-1}$ with $D_s^{-1}=\beta_s m$ in which

$$\beta_s = \frac{1}{1+e}\frac{\partial e}{\partial(p_g - p_w)} \tag{35}$$

$C_T = D\,D_t^{-1}$ with $D_t^{-1} = \beta_t m$ in which

$$\beta_t = \frac{1}{1+e}\frac{\partial e}{\partial(T)} \tag{36}$$

$L_C = DD_c^{-1}$ with $D_c^{-1}= \beta_t m$ in which

$$\beta_c = \frac{1}{1+e}\frac{\partial e}{\partial(C)} \tag{37}$$

and

$$m=[1\ 1\ 0] \tag{38}$$

Void ratio and degree of saturation in unsaturated soil depend on the total stress, suction and temperature (e.g. Fredlund, 1979; Lloret and Alonso, 1985; Sultan et al., 1997; Gatmiri, 1997). Continuing these works to consider the effect of chemical concentration, these surfaces are suggested here for degree of saturation and void ratio:

$$S_r = 1-[a_s + b_s(\sigma - p_g)][1-\exp(c_s(p_g - p_w))]$$
$$\exp(f_s(C-C_0))\exp(d_s(T-T_0)) \tag{39}$$

and :

$$e = \frac{(1+e_0)\exp[-c_e(T-T_0)]}{\exp\left(\left[a_e(\frac{\sigma-p_g}{p_{atm}}) + b_e(1-\frac{\sigma-p_g}{\sigma_c})(\frac{p_g-p_w}{p_{atm}}) + d_e(1-\frac{\sigma-p_g}{\sigma_c})(\frac{RT(C-C_0)}{p_{atm}})\right]^{1-m}/K_b(1-m)\right)} - 1 \tag{40}$$

Where σ is the mean stress, σ_c preconsolidation stress, T_0 initial temperature, C_0 initial concentration, K_b, m, a_e, b_e, c_e, d_e, as, b_s, c_s, $d_s$and f_s are the parameters of void ratio and degree of saturation state surfaces. Figure 1 shows an example of void ratio surface in the case where the mean stress and the temperature have been fixed hence void ratio is function of suction and concentration of chemical species.

We assume consistency and convergence of finite element discretization in space (Zienkiewicz and Taylor, 1989). The formulation outlined above has been discretized in order that it can be used in the finite element analysis. The weighted residual method with the Galerkin choice of weighted functions was applied for spatial discretization of domain W. Terms involving second spatial derivatives are transformed by means of Gauss's theorem. In this discretization conveniently the same element shape functions are used for all variables, though not necessarily identical interpolations, especially when approaching the undrained limit state (e.g. Zienkiewicz et al. 1990).

The single-step integration (q method) was used for time discretization. The global matrix form of equations was encoded and solved in finite element program. FEM is not locally mass conservative. In this paper, convective velocity in unsaturated media is small so using a fine mesh, the error in mass conservation is small and can be neglected.

The final matrix form is as follows:

$$\begin{bmatrix} [R] & [C_w] & [C_g] & [C_T] & [C_s] \\ [C_{wu}] & [C_{ww}] & [C_{wg}] & [C_{wT}] & [C_{ws}] \\ [C_{gu}] & [C_{gw}] & [C_{gg}] & [C_{gT}] & [C_{gs}] \\ [C_{Tu}] & [C_{Tw}] & [C_{Tg}] & [C_{TT}] & [C_{Ts}] \\ [C_{su}] & [C_{sw}] & [C_{sg}] & [C_{sT}] & [C_{ss}] \end{bmatrix} \begin{Bmatrix} \dot{u} \\ \dot{P}_w \\ \dot{P}_g \\ \dot{T} \\ \dot{C} \end{Bmatrix} + \begin{bmatrix} [0] & [0] & [0] & [0] & [0] \\ [0] & [K_{ww}] & [K_{wg}] & [K_{wT}] & [K_{ws}] \\ [0] & [K_{gw}] & [K_{gg}] & [K_{gT}] & [K_{gs}] \\ [0] & [K_{Tw}] & [K_{Tg}] & [K_{TT}] & [K_{Ts}] \\ [0] & [K_{sw}] & [K_{sg}] & [K_{sT}] & [K_{ss}] \end{bmatrix} \begin{Bmatrix} u \\ P_w \\ P_g \\ T \\ C \end{Bmatrix} = \begin{Bmatrix} \{\dot{F}_\sigma\} \\ F_w \\ F_g \\ F_T \\ F_s \end{Bmatrix} \tag{41}$$

in which mechanical terms of coupling are:

$$\begin{aligned} [\mathrm{R}] &= \int_\Omega \mathrm{B}^{\mathrm{T}} \mathrm{D} \mathrm{B} \mathrm{d}\Omega \\ [\mathrm{C_w}] &= \int_\Omega \mathrm{B}^{\mathrm{T}} \mathrm{F} \mathrm{N} \mathrm{d}\Omega \\ [\mathrm{C_g}] &= \int_\Omega \mathrm{B}^{\mathrm{T}} (\mathbf{m} - \mathrm{F}) \mathrm{N} \mathrm{d}\Omega \\ [\mathrm{C_T}] &= \int_\Omega \mathrm{B}^{\mathrm{T}} \mathrm{C_T} \mathrm{N} \mathrm{d}\Omega \\ [\mathrm{C_c}] &= \int_\Omega \mathrm{B}^{\mathrm{T}} \mathrm{L_c} \mathrm{N} \mathrm{d}\Omega \\ \{\mathrm{F}_\sigma\} &= \int_\Gamma \mathrm{N}^{\mathrm{T}} \bar{\sigma} \mathrm{d}\Gamma + \int_\Omega \mathrm{N}^{\mathrm{T}} \dot{\mathrm{b}} \mathrm{d}\Omega \end{aligned} \tag{42}$$

water pressure terms of coupling are :

$$\begin{aligned} [\mathrm{K_{ww}}] &= \int_\Omega (\nabla \mathrm{N})^{\mathrm{T}} \mathrm{D_p} (\nabla \mathrm{N}) \mathrm{d}\Omega \\ [\mathrm{K_{wg}}] &= \int_\Omega (\nabla \mathrm{N})^{\mathrm{T}} \mathrm{D_{p'}} (\nabla \mathrm{N}) \mathrm{d}\Omega \\ [\mathrm{K_{wT}}] &= \int_\Omega (\nabla \mathrm{N})^{\mathrm{T}} \mathrm{D_T} (\nabla \mathrm{N}) \mathrm{d}\Omega \\ [\mathrm{K_{ws}}] &= \int_\Omega (\nabla \mathrm{N})^{\mathrm{T}} \mathrm{D_c} (\nabla \mathrm{N}) \mathrm{d}\Omega \end{aligned} \tag{43}$$

and

$$\begin{aligned} [\mathrm{C_{wu}}] &= \int_\Omega \mathrm{N}^{\mathrm{T}} (\mathbf{c_{wu}} + \mathrm{b_{f1}} (1-\mathrm{n}) \mathrm{m}^{\mathrm{T}}) \mathrm{d}\Omega \\ [\mathrm{C_{ww}}] &= \int_\Omega \mathrm{N}^{\mathrm{T}} \mathbf{c_{ww}} \mathrm{N} \mathrm{d}\Omega \\ [\mathrm{C_{wg}}] &= \int_\Omega \mathrm{N}^{\mathrm{T}} \mathbf{c_{wg}} \mathrm{N} \mathrm{d}\Omega \\ [\mathrm{C_{wT}}] &= \int_\Omega \mathrm{N}^{\mathrm{T}} \mathbf{c_{wT}} \mathrm{N} \mathrm{d}\Omega \\ [\mathrm{C_{ws}}] &= \int_\Omega \mathrm{N}^{\mathrm{T}} \mathbf{c_{ws}} \mathrm{N} \mathrm{d}\Omega \\ \{\mathrm{F_w}\} &= -\int_\Gamma \mathrm{N}^{\mathrm{T}} (\bar{\mathrm{q}}_{\mathrm{w}} + \bar{\mathrm{q}}_{\mathrm{v}}) \mathrm{d}\Gamma - \int_\Omega \nabla \mathrm{N}^{\mathrm{T}} (\mathrm{D_w}) \nabla \mathrm{Z} \mathrm{d}\Omega \end{aligned} \tag{44}$$

gas pressure terms of coupling are:

$$\begin{aligned} [\mathrm{K_{gw}}] &= \int_\Omega (\nabla \mathrm{N})^{\mathrm{T}} \mathrm{D_{2p}} (\nabla \mathrm{N}) \mathrm{d}\Omega \\ [\mathrm{K_{gg}}] &= \int_\Omega (\nabla \mathrm{N})^{\mathrm{T}} \mathrm{D_{2p'}} (\nabla \mathrm{N}) \mathrm{d}\Omega \\ [\mathrm{K_{gT}}] &= \int_\Omega (\nabla \mathrm{N})^{\mathrm{T}} \mathrm{D_{2T}} (\nabla \mathrm{N}) \mathrm{d}\Omega \\ [\mathrm{K_{gs}}] &= \int_\Omega (\nabla \mathrm{N})^{\mathrm{T}} \mathrm{D_{2c}} (\nabla \mathrm{N}) \mathrm{d}\Omega \end{aligned} \tag{45}$$

and

$$\begin{aligned} [\mathrm{C_{gu}}] &= \int_\Omega \mathrm{N}^{\mathrm{T}} (\mathbf{c_{gu}} + \mathrm{a_{f3}} (1-\mathrm{n}) \mathrm{m}^{\mathrm{T}}) \mathrm{d}\Omega \\ [\mathrm{C_{gw}}] &= \int_\Omega \mathrm{N}^{\mathrm{T}} \mathbf{c_{gw}} \mathrm{N} \mathrm{d}\Omega \\ [\mathrm{C_{gg}}] &= \int_\Omega \mathrm{N}^{\mathrm{T}} \mathbf{c_{gg}} \mathrm{N} \mathrm{d}\Omega \\ [\mathrm{C_{gT}}] &= \int_\Omega \mathrm{N}^{\mathrm{T}} \mathbf{c_{gT}} \mathrm{N} \mathrm{d}\Omega \\ [\mathrm{C_{gs}}] &= \int_\Omega \mathrm{N}^{\mathrm{T}} \mathbf{c_{gs}} \mathrm{N} \mathrm{d}\Omega \\ \{\mathrm{F_g}\} &= -\int_\Gamma \mathrm{N}^{\mathrm{T}} \bar{\mathrm{q}}_{\mathrm{g}} \mathrm{d}\Gamma - \int_\Omega \nabla \mathrm{N}^{\mathrm{T}} (\mathrm{D_{2w}}) \nabla \mathrm{Z} \mathrm{d}\Omega \end{aligned} \tag{46}$$

thermal terms of coupling are:

$$\begin{aligned} [K_{Tw}] &= \int_\Omega (\nabla N)^T [(T-T_0)(\mathrm{C_{pw}} \rho_w D_{\rho w} + \mathrm{C_{pv}} \rho_w D_{\rho v} \\ &+ \mathrm{C_{pc}} M_c C D_{\rho w}) + h_{fg} D_{\rho v} \rho_w] (\nabla N) \mathrm{d}\Omega \\ [K_{Tg}] &= \int_\Omega (\nabla N)^T) [(T-T_0)(-\mathrm{C_{pw}} \rho_w D_{\rho w} - \mathrm{C_{pv}} \rho_w D_{\rho v} \\ &+ K_g (\mathrm{C_{pa}} \rho_a + \mathrm{C_{pv}} \rho_v) / \gamma_g - \mathrm{C_{pc}} M_c C D_{\rho w}) - h_{fg} D_{\rho v} \rho_w \\ &+ h_{fg} K_g / \gamma_g] (\nabla N) \mathrm{d}\Omega \\ [K_{TT}] &= \int_\Omega (\nabla N)^T) [(T-T_0)(-\mathrm{C_{pw}} \rho_w D_{Twc} + \mathrm{C_{pv}} \rho_w D_{Tv} \\ &- \mathrm{C_{pc}} M_c C D_{Twc}) - h_{fg} D_{Tv} \rho_w + \lambda] (\nabla N) \mathrm{d}\Omega \\ [K_{Ts}] &= \int_\Omega (\nabla N)^T) [(T-T_0)(-\mathrm{C_{pw}} \rho_w D_{cw} \\ &+ \mathrm{C_{pc}} M_c (C D_{cw} + \theta D_{duff}))] (\nabla N) \mathrm{d}\Omega \end{aligned} \tag{47}$$

and

$$\begin{aligned} [C_{Tu}] &= \int_\Omega N^T (\mathrm{c_{Tu}} + c_{f4} (1-n) m^T) \mathrm{d}\Omega \\ [C_{Tw}] &= \int_\Omega N^T \mathrm{c_{Tw}} N \mathrm{d}\Omega \\ [C_{Tg}] &= \int_\Omega N^T \mathrm{c_{Tg}} N \mathrm{d}\Omega \\ [C_{TT}] &= \int_\Omega N^T \mathrm{c_{TT}} N \mathrm{d}\Omega \\ [C_{Ts}] &= \int_\Omega N^T \mathrm{c_{Ts}} N \mathrm{d}\Omega \\ \{F_T\} &= -\int_\Gamma N^T \bar{q}_h d\Gamma - [(\mathrm{T} - \mathrm{T_0})(\mathrm{C_{pw}} \rho_w K_w \\ &+ K_g (\mathrm{C_{pa}} \rho_a + \mathrm{C_{pv}} \rho_v) + \mathrm{C_{pc}} M_c C K_w) + h_{fg} \rho_v K_g] \nabla \mathrm{Z} \mathrm{d}\Omega \end{aligned} \tag{48}$$

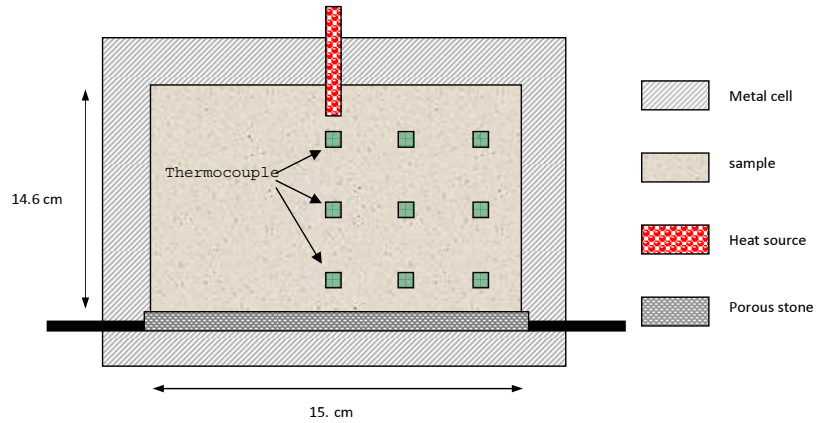

Fig. 2 Schematic diagram of heat transfer cell (Villar et al., 1993)

and chemical terms of coupling

$$
\begin{aligned}
[K_{sw}] &= \int_{\Omega} (\nabla N)^T \mathrm{D}_{3\mathrm{p}} (\nabla N) \mathrm{d}\Omega \\
[K_{sg}] &= \int_{\Omega} (\nabla N)^T \mathrm{D}_{3\mathrm{p}'} (\nabla N) \mathrm{d}\Omega \\
[K_{sT}] &= \int_{\Omega} (\nabla N)^T \mathrm{D}_{3\mathrm{T}} (\nabla N) \mathrm{d}\Omega \\
[K_{ss}] &= \int_{\Omega} (\nabla N)^T \mathrm{D}_{3\mathrm{c}} (\nabla N) \mathrm{d}\Omega
\end{aligned}
\qquad (49)
$$

and :

$$
\begin{aligned}
[C_{su}] &= \int_{\Omega} N^T (\mathbf{c}_{\mathrm{su}} + CS_r(1-n)) \mathrm{d}\Omega \\
[C_{sw}] &= \int_{\Omega} N^T \mathbf{c}_{\mathrm{sw}} N \mathrm{d}\Omega \\
[C_{sg}] &= \int_{\Omega} N^T \mathbf{c}_{\mathrm{sg}} N \mathrm{d}\Omega \\
[C_{sT}] &= \int_{\Omega} N^T \mathbf{c}_{\mathrm{sT}} N \mathrm{d}\Omega \\
[C_{ss}] &= \int_{\Omega} N^T (\theta + \mathbf{c}_{\mathrm{ss}}) N \mathrm{d}\Omega \\
\{F_s\} &= \int_{\Gamma} N^T \bar{q}_{\theta c} d\Gamma - \int_{\Omega} \nabla N^T (\mathrm{CK}_{\mathrm{w}}) \nabla Z \mathrm{d}\Omega
\end{aligned}
\qquad (50)
$$

For further details, see Ghasemzadeh (2006).

Application and results

Above theories of Thermo-Hydro-Chemo-Mechanical coupling have been applied in two-dimensional finite element code. The objective of this section is the verification of above formulation and code to estimate thermal transport and solute transport in soil. One heat transport and two examples containing sodium chloride transport and soil/solute interaction in unsaturated media are presented here.

Heat transfer

In the first example, the thermo-hydraulic behaviour of undeformable partially saturated soils will be verified. Results of the application of this model to a laboratory test by Villar et al. (1993) is presented hereafter. The required parameters have been determined from experimental results and are as the following:

A montmorillonite clay sample has been uniaxially compacted in a stainless steel cell which has a height of 14.6 cm and an inner diameter of 15 cm to a dry density of 1.62 g/cm^3. A heater has been placed at the center of the upper part of the cylinder and heated up to 100°C. Nine thermocouples measure the temperature distribution at different levels. The temperature along the external boundary of the cell is kept constant, about 25-30°C, by a warm shower. At the end of each test, the sample has been taken out and cut, in order to measure the water content and dry density. The overall configuration is shown in Fig. 2. All dimensions are in cm. Since the finite element package is written under assumption of plain strain, a vertical section of cylindrical cell is considered. The finite element mesh used in this application is four nodes isoparametric elements. There isn't solute transfer in this example so the solute concentration is zero for all nodes. The following boundary conditions are chosen

Table 1 Physical characteristics of the medium

Properties	Unit	Values
Initial degree of saturation	$S_r(Cm^3/Cm^3)$	0.5
Porosity	$n(Cm^3/Cm^3)$	0.73
Density of grain	$\rho(kg/m^3)$	2780
Calorific capacity of soil grain	C_{ps} (J/kg°C)	800
Calorific capacity of water	C_{pw} (J/kg°C)	4180
Calorific capacity of vapour	C_{pv} (J/kg°C)	1870
Calorific capacity of air	C_{pg} (J/kg°C)	1000
Thermal conductivity of soil grain	λ_s (W/m°C)	0.9
Thermal conductivity of water	λ_w (W/m°C)	0.6
Thermal conductivity of gas	λ_g (W/m°C)	0.0258
Latent heat of evaporation	h_{fg}(J/kg)	2.40×10^6

(Villar et al., 1993).

temperature of 28°C on all nodes on the outer boundaries of the soil sample and 100°C for heater, all boundaries are impermeable relative to moisture movement, all boundaries are impermeable relative to air transfer except the upper boundary for which a permeable boundary is defined, the vertical displacement of the bottom of the cell is fixed at zero and the horizontal displacements of the lateral boundaries are also fixed at zero. The initial conditions are; $T_0 = 20°C$, $S_r = 0.5$ and $e_0 = 0.73$. The initial suction is defined via the state surface of degree of saturation by using the value of degree of saturation. Based on experimental works, the other parameters used in this numerical test are chosen as noted in Table 1. Water and gas permeability in terms of void ratio and degree of saturation are as following (Villar et al., 1993):

$$K_w = 1.2\times10^{-9}.10^{5e}\left(\frac{S_r - 0.05}{0.95}\right)^3\left(\frac{64.15}{T-229}\right)^{-1.562} \quad \text{m/s} \quad (51)$$

$$K_g = \frac{3\times10^{-10}\gamma_g}{1.846\times10^{-5}}[e(1-S_r)]^4 \quad \text{m/s} \quad (52)$$

Void ratio and degree of saturation surface are assumed as following:

$$e = \frac{1.73}{\exp\left[\frac{[1.5(\frac{\sigma-p_g}{p_{atm}}) + 0.15(1-\frac{\sigma-p_g}{80\times10^4})(\frac{p_g-p_w}{p_{atm}})]}{33}\right]\exp[-3\times10^{-4}(T-T_0)]} - 1 \quad (53)$$

$$S_r = 1-[1.0+(-2.088\times10^{-8})(\sigma-p_g)] \quad (54)$$

$$[1-\exp((-2.08855\times10^{-4})(p_g-p_w))]\exp(10^{-5}(T-T_0))$$

At the end of the test after two hours, the calculated results of temperature, degree of saturation, void ratio and suction are presented in the figure 3 to figure 6, respectively. Experimental results are also presented in the figure 3 to 5 with a triangle sign. A comparison between calculated and experimental results shows relatively good agreement.

Chloride solution transport

The second example is validation of solute dispersion in unsaturated medium without any chemical reaction. For this purpose, the experiments of Nützmann et al. (2002) on unsaturated glass beads were used.

In these experiments, a column of 100 cm height and 20.6 cm internal diameter filled of glass

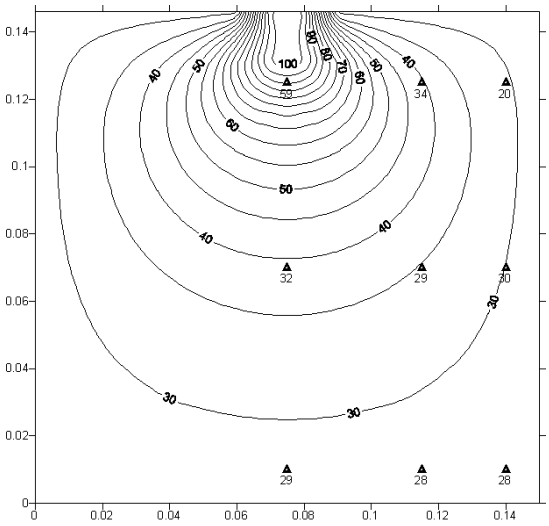

Fig. 3 Experimental (Villar et al., 1993) and calculated temperature

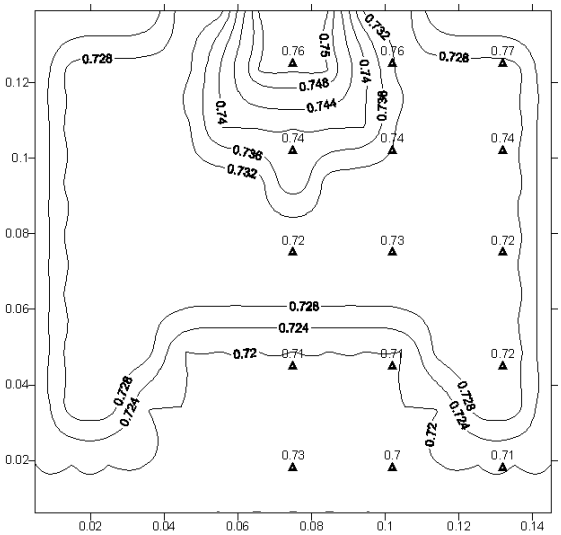

Fig. 5 Experimental (Villar et al., 1993) and calculated void ratio

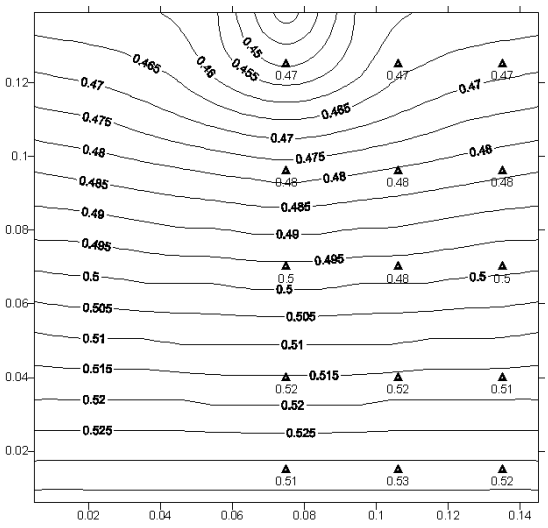

Fig. 4 Experimental (Villar et al., 1993) and calculated degree of saturation

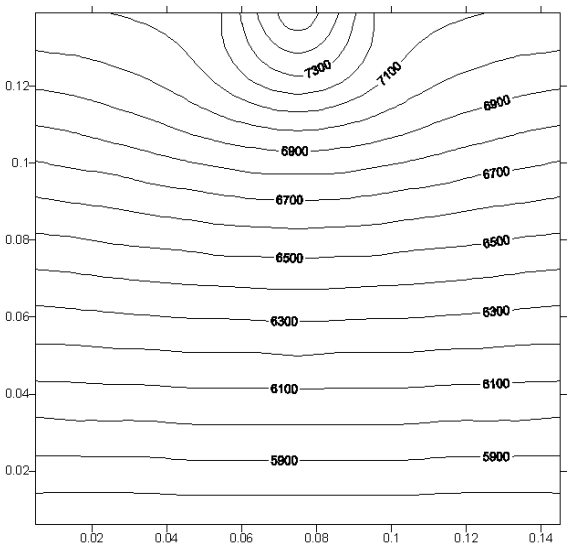

Fig. 6 Calculated suction in present study

Table 2 Physical characteristics of the medium

Properties	Unit	Values
Porosity	n (cm^3/cm^3)	0.347
Particle density	ρ (kg/dm^3)	2.57
Saturated hydraulic conductivity	K_s (cm/s)	0.0794
Volumetric water content	θ (cm^3/cm^3)	0.14
Infiltration rate	q_{inf} (cm/s)	0.009867
Initial sorbent concentration	C_s (g/l)	0.06

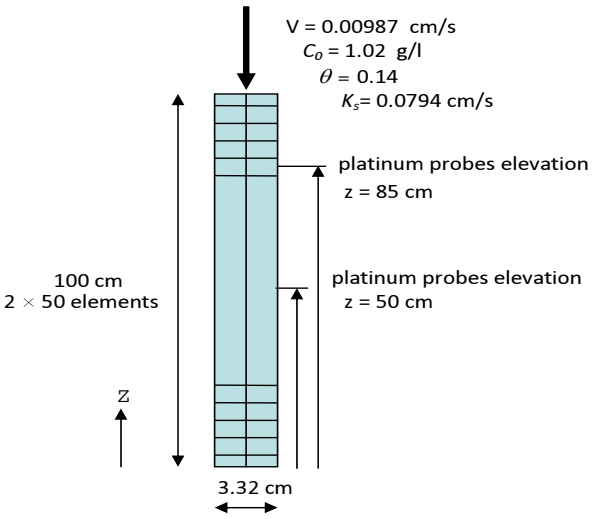

Fig. 7 Geometry of example 2

beads has been used. The glass beads had particle sizes ranging from 0.36 to 0.71 mm in diameter with the properties presented in Table 2. Each displacement experiment has been begun with a constant water infiltration. The tracer was injected after steady state water flow through the column was reached; thus there is no hysteresis problem. Experiments have been carried out for different infiltration rates, where the calculated molecular Peclet numbers were between 40<Pemol<600, indicating that mass flux was dominated by dispersion with negligible diffusion (Pfannkuch, 1963; Van Genuchten and Wierenga, 1976). All experiments have been repeated three times.

Three platinum probes were placed at each depth with an angle of 120° between them to measure concentration. The breakthrough curves measured at 15 cm (z=85 cm) and 50 cm (z= 50 cm) distances from the top of the column are presented in Figure 8. The difference between the results of different probes in the same level is due to high fluctuation of water velocity in the unsaturated medium (Nützmann et al., 2002).

In the numerical study, a mesh of 2 × 50 rectangular elements was used which is presented in the figure 7. Total height is 100 cm and section area is 100 × 3.32 cm² which is section surface of experiment column. The tracer (Nacl) with a concentration of 1.02 g/l was injected to the top of column after a steady state infiltration of water. The duration of the experiment was approximately two hours and half. Longitudinal dispersivity coefficient was considered as (Nützmann et al., 2002):

$$\alpha_L = 0.00395\theta^{-2.89689} \tag{55}$$

The calculated breakthrough curves at z=85 cm and z= 50 cm distances are also given in the figure 8. At z=0.85 the concentration starts to increase from initial value (C_s= 0.06 g/l) after about 120seconds and it reaches to entrance concentration (C=1.02 g/l) after about 500 seconds. At z=0.50 the concentration starts to increase from initial value after about 450 seconds and it reaches to entrance concentration after about 1250 seconds. We observe that these calculated results in different depths are among the results obtained from different probes at the same depth. Figure 9 shows comparison of the calculated results and average of measured tracer breakthrough curves in each level. A good agreement can be seen between average of experimental results and these of numerical simulations.

Solute transfer and soil deformation

Soil deformation due to solute transfer in unsaturated medium is presented in this example.

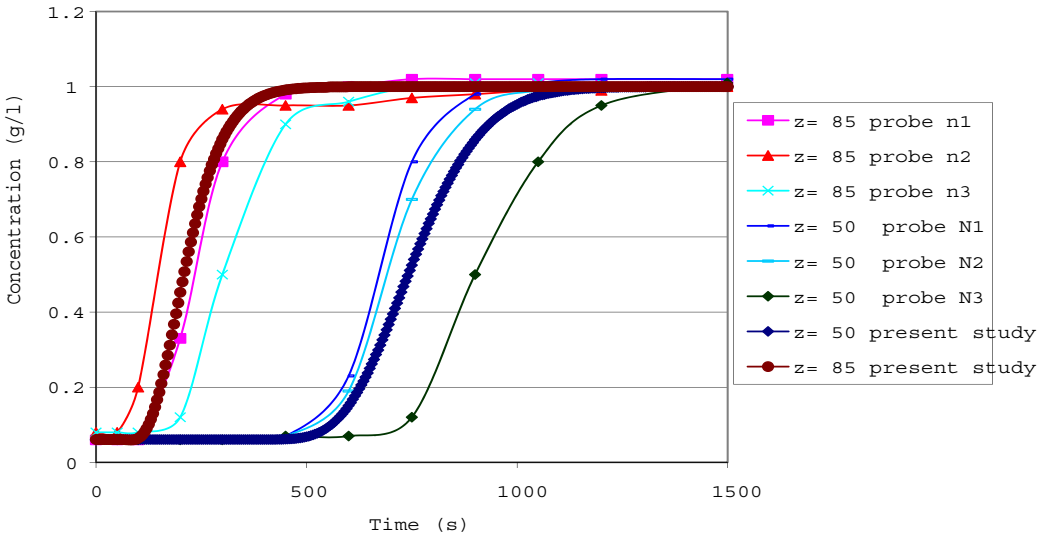

Fig. 8 Measured tracer breakthrough curves in unsaturated glass beads for different probes from Nützmann et al. (2002) and results of present study.

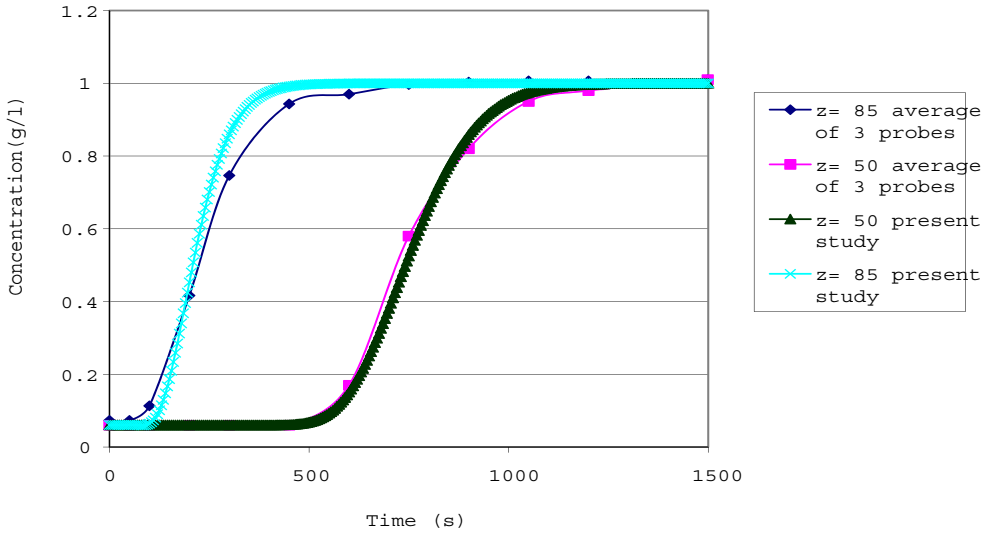

Fig. 9 Comparison of present study results and average of measured tracer breakthrough curves in unsaturated glass beads from Nützmann et al. (2002).

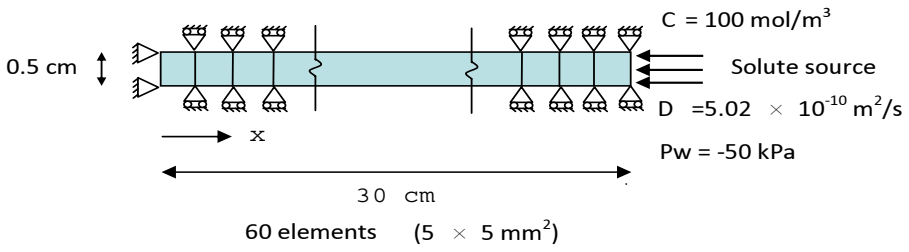

Fig. 10 Geometry of example 3

Table 3 Physical characteristics of the soil and solute

Properties	Unit	Values
Hydraulic Conductivity	K (m/s)	1×10^{-12}
Porosity	n(cm^3/cm^3)	0.33
Initial degree of saturation	S_r	0.60
Temperature	T(°C)	20
Solute dispersion Coefficient	D (m^2/c)	5.02×10^{-10}
Molecular mass of solute	M (gr/mol)	58.5
Bulk density	ρ (kg/dm^3)	1.5
Osmotic Efficiency	ω	0.3

An unsaturated specimen with constant osmotic efficiency equal to 0.3 is subjected to solute transfer. Solute source was placed in the right boundary of the soil sample with 30 cm width and 0.5 cm height. The mesh consists of 60 four-node elements (Figure 10). We suppose that there is no solute sorption therefore only the solute transfer is considered. The concentration of solute in the right boundary is 100 mol/m^3. Initial water pressure and initial air pressure are -50 kPa and zero, respectively. All nodes were restricted against vertical displacement . all nodes can move horizontally except nodes on left boundary. Boundary conditions for the problem are shown in Figure 10. Soil and solute characteristics are presented in Table 3. Void ratio and degree of saturation surface equations are as followings:

$$e = \frac{1.49\exp[-.9\times10^{-6}(T-T_0)]}{\exp\left[\frac{[0.1(\frac{\sigma-p_g}{p_{atm}})+0.1(1-\frac{\sigma-p_g}{80\times10^4})(\frac{p_g-p_w}{p_{atm}})]}{25}\right]}-1 \quad (56)$$

$$S_r = 1-[1.0+(-2\times10^{-8})(\sigma-p_g)]$$
$$[1-\exp(10^{-5}(p_g-p_w))]\exp(10^{-5}(T-T_0)) \quad (57)$$

Concentration of dissolved solute in water is presented in Figure 11. At source point (x=30 cm), concentration is always equal to 100 mol/m^3 and concentration of the other points reach to this value after about ten years. For a given time, concentration increases sharply near by source point and it increases more slowly far from source point. The further the distance from source point, the later the concentration increases. For example, concentration at x=20 cm reaches to 60 mol/ m^3 after one year, while at x=0, it lasts more than three year for reaching to this concentration. Degree of saturation and water pressure in different distance are presented in Figure 12 and Figure 13, respectively. These figures show that there is a flow of water toward source of solute while there is solute flow toward the other end of specimen. Figure 13 shows increase of water pressure beside source of solute (x=30, x=25, x=20) and decrease of water pressure far from solute source (x=0, x=5, x=10). In the beginning of diffusion, solute concentration is high near the source and it is low far from this region. Having equal free energy of solution in different points of specimen, water moves toward solute source therefore degree of saturation increases in this part of specimen. In other word, solute diffusion generates water pressure in the medium because of none zero osmotic efficiency.

Diffusion of solute in medium is completed after about ten years and all nodes reach to the same concentration. In this condition, degree of saturation of all nodes reach to 0.60 that is initial value and water pressure also reaches to its initial value (P_w = 50 kPa).

Variation of water pressure results in deformation of specimen that is presented in Figure 14 and Figure 15. Deformation in different nodes increases until about one year then deformation

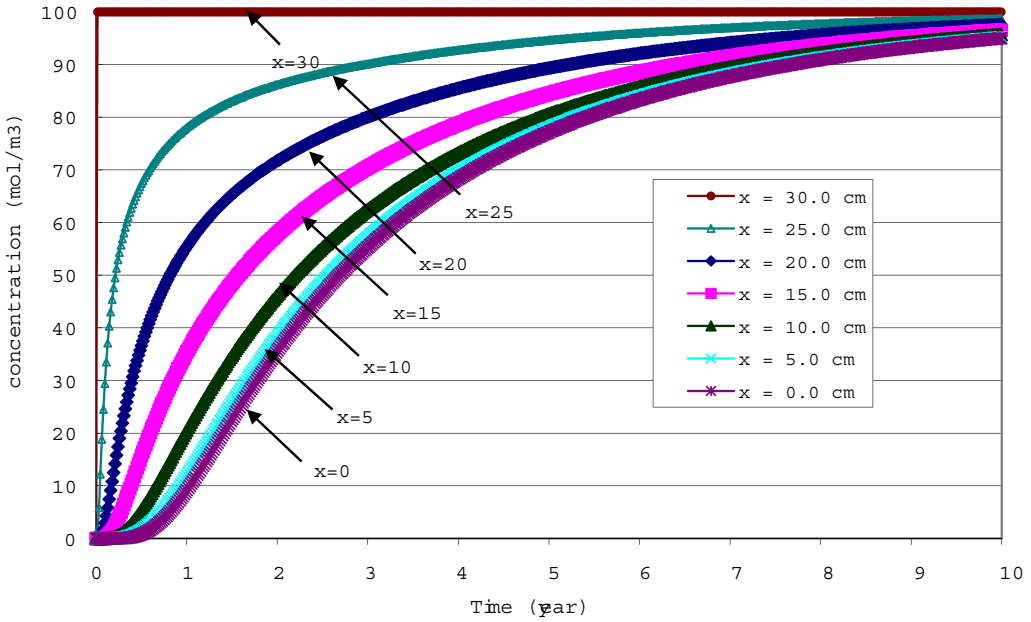

Fig. 11 Variation of solute concentration in different distances.

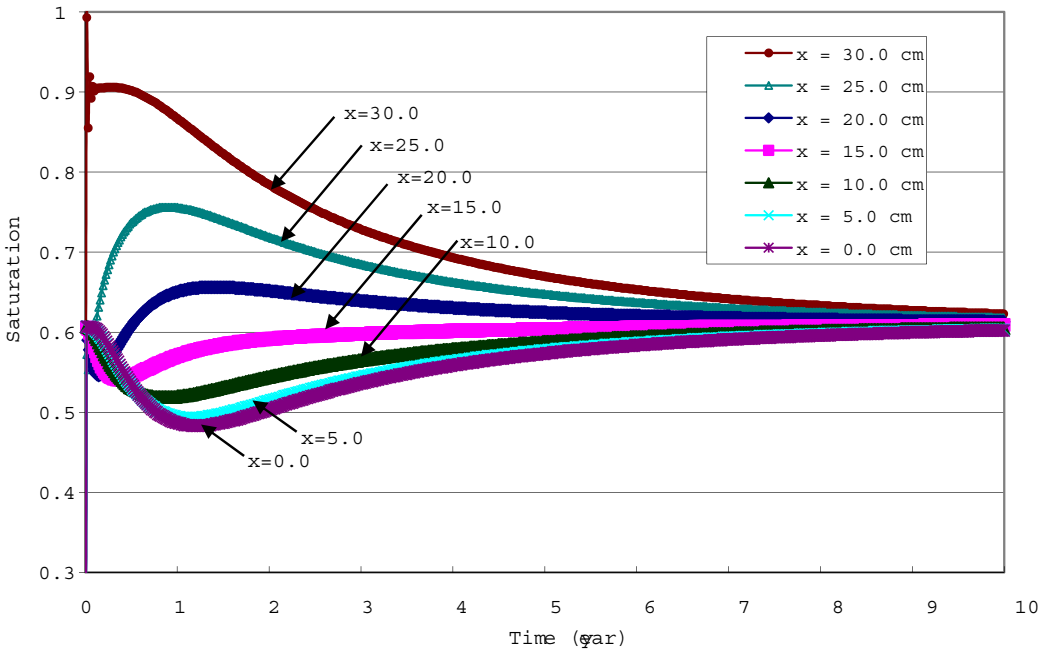

Fig. 12 Variation of saturation degree in different distances.

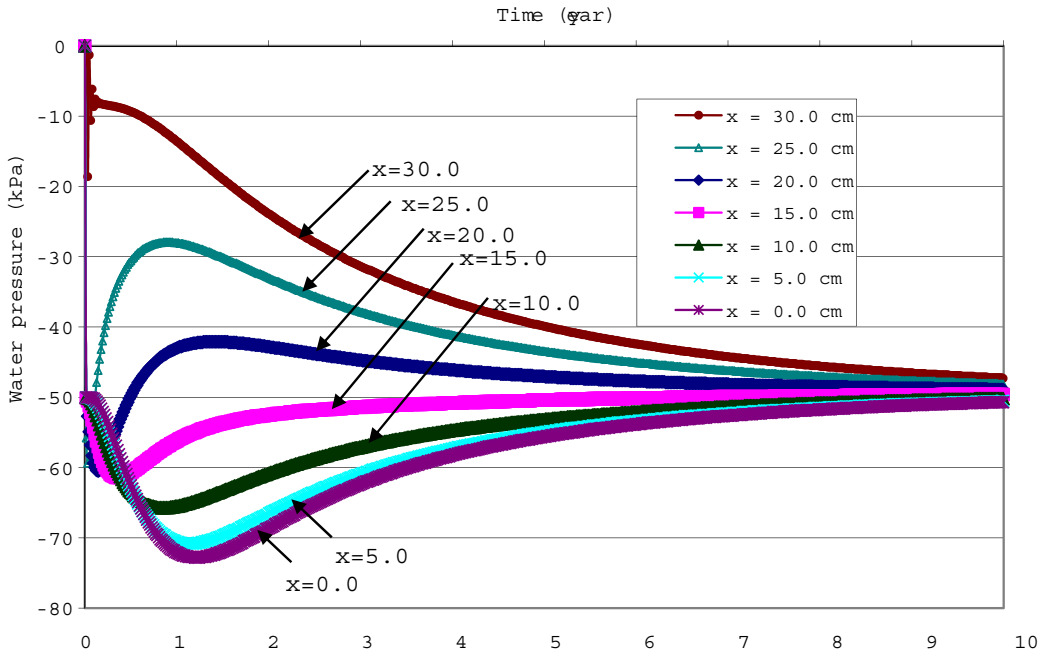

Fig. 13 Variation of water pressure in different distances.

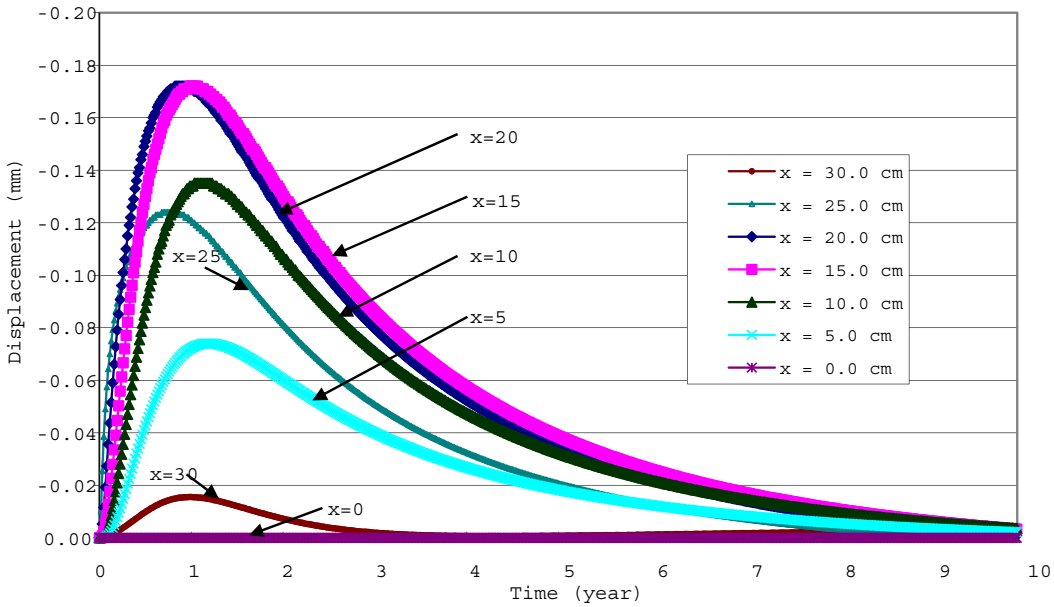

Fig. 14 Soil displacement in different nodes

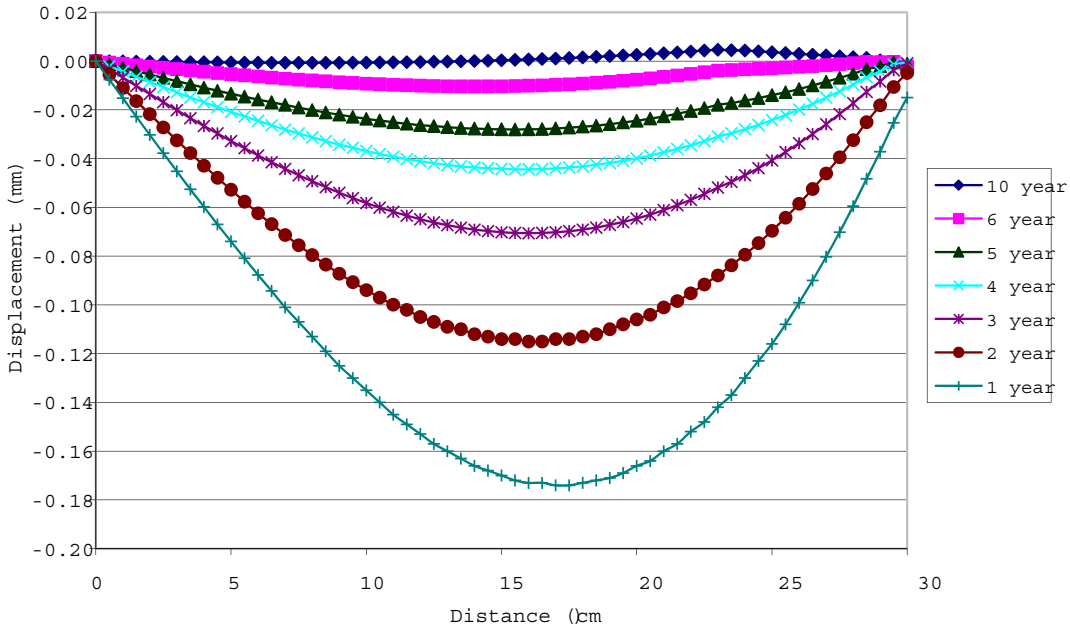

Fig. 15 Soil displacement of specimen in different times

decreases. After one year, maximum of displacement is about 0.17 mm at x=18 cm which is more than maximum displacement at x=30 cm is about than 0.02 mm (Figure 15). These results show that deformation consists of contraction and expansion in the soil sample. This deformation occurs due to change of suction in nodes. As noted in Figure 12 and Figure 13, there is movement of water toward solute source and so decreasing of water pressure or increasing of suction. This suction results in contraction in points that are far from solute source. On the other hand, in the region near the solute source expansion occurs because of diminution of suction due to generation of osmotic pressure in this region.

Conclusion

In this paper the transfer of heat and mass in the deformable porous media was studied and a new set of formulation to express heat and mass transfer was presented. Mechanical properties and heat/mass transfer in medium is totally coupled trough this formulation. This formulation was integrated into one finite element code. Three examples were explained for validation and application of this formulation. The results of heat transfer and chemical species transfer were compared with experimental ones. The comparison of the present study results and the experimental ones showed a good agreement. The results show capacity of presented formulation for simulation of heat and mass transfer in deformable porous media. More development can be done to model for considering chemical reactions in this formulation.

Nomenclature

σ' : effective stress
σ : total stress
ε : deformation tensor
D : stiffness matrix
P_g : gas pressure
P_w : water pressure
s : suction (s = P_g-P_w)
P_{atm} : atmospheric pressure
T : temperature

C : solute concentration
M_c : molar mass of contaminant
θ : volumetric water content
v : pore water velocity
e : void ratio
n : porosity
S_r : degree of saturation
U : water velocity
V_v : vapor velocity
D : hydrodynamic dispersion tensor
D_m : molecular diffusion coefficient
D^* : effective molecular diffusion coefficient
D_{disp} : mechanic dispersion coefficient
τ : tortuosity
K_b : Boltzmann constant
a_L : longitudinal dispersion coefficient
a_T : transversal dispersion coefficient
P_e : Peclet number
ρ_b: : aquifer apparent density
erf : error function
$erfc$: complimentary error function
δ_{ij} : Kronecker symbol (ij = 1 if i=j and 0 otherwise)
ψ : thermodynamic potential
ψ_m : matrix potential
ψ_o : osmotic potential
ρ_w : water density
ρ_g : gas density
ρ_s : soil density
h : relative humidity
K_w : water permeability
K_g : air permeability
h_{fg} : latent heat
μ_w : viscosity of water
μ_g : viscosity of gas
λ : thermal conductivity of media
λ_w : thermal conductivity of water
λ_v : thermal conductivity of vapor
λ_a : thermal conductivity of air
λ_c : thermal conductivity of solute
H : solubility coefficient of gas in water (Henry constant)
C_T : total heat capacity of media
C_{Pw} : specific heat capacity of water
C_{Pv} : specific heat capacity of vapor
C_{Pg} : specific heat capacity of gas
C_{Pc} : specific heat capacity of solute
R : universal constant of gas
P_{os} : osmotic pressure
ω : osmotic efficiency

Reference

[1] Barbour S.L., and Fredlund D.G. 1989. Mechanisme of osmotic flow and volume change in clay soils. Canadian Geothecnical Journal. 26 : 551-562.

[2] Bear J. 1979. Hydraulics of groundwater McGraw-Hill, New York. 210 pp.

[3] Bresler E. 1973. Anion exclusion and coupling effects in nonsteady transport through unsaturated soils: I. Theory. Soil Sci. Soc. Am. Proc. 37:663-669.

[4] Corey A.T. 1957. Measurement of water and air permeability in unsaturated soil. Soil Sci. Soc. Amer. Proc. 21, 7-10

[5] Farouki O. T. 1986. Thermal properties of soil. Trans. Tech. Publications, Allemagne.

[6] Fetter C.W. 1993. Contaminant Hydrogeology. Prentice Hall, second edition, New Jersey.

[7] Fredlund D.G. 1979. Appropriate concepts and technology for unsaturated soils. Canadian geotech. J. 16, 121-139.

[8] Gardner W.R. 1958. Some steady state solutions of the unsaturated moisture flow equation with application to evaporation from a water-table. J. Soil Science, 85(4) 228-232.

[9] Gatmiri B. 1997. Analysis of fully coupled behavior of unsaturated porous media under stress, suction and temperature gradient. Rapport final for CERMES-ENPC, Mars 1997.

[10] Gatmiri B., Jenab-Vossoughi B, and Delage P. 1999. Validation of -STOCK, A finite element software for the analysis of thermo-hydro mechanical behaviour of engineering clay barriers, in Proc. Of the NAFEMS World Congress, Volume 1, Newport, Rhode Island, Etats-Unis, pp. 645-656.

[11] Gens A., Alonso E.E. and Delage P. 1997.

Computer modeling and applications in unsaturated soils. in Houston S.L. et Fredlund D.G. (Ed.). Unsaturated soil engineering practice 299-330, ASCE.

[12] Gens A., Olivella S. 2000. Non isothermal multiphase flow in deformable porous media. Coupled formulation and application to nuclear waste disposal. In development in theoritical geomechanics, Smith & Carter 5Eds.), Balkema, Roterdam, pp. 619-640.

[13] Gens A., Olivella S. 2001. THM phenomena in saturated and unsaturated porous media. Revue française de génie civil, volume 5 n°6/2001. 694-717.

[14] Gens A., Leonardo N.G. and Olivella S. 2002. Coupled chemomechanical analysis for saturated and unsaturated soils. In Environmental geomechanics ed. Vulliet L., Laloui L. and Schrefler B. Switzerland.

[15] Ghasemzadeh H. 2006. Couplages dans les geomateriaux multiphasiques effets de la température et de la chimie. Thèse de doctorat :l'Ecole Nationale des Ponts et Chaussées, 203p.

[16] Greenkorn R.A., Kessler D.P. 1972. Transfer Operations. McGraw-Hill, New York.

[17] Irmay S. 1954. On the hydraulic conductivity of unsaturated soils. Trans. Amer. Geophys. Uni. 35, 463-468

[18] Kovacs G. 1981, Seepage hydraulics. Amesterdam, Pays-Bas; Elsevier Science Publishers B.V.

[19] Langfelder L.J., Chen C.F. and Justice J.A. 1968. Air permeability of compacted cohesive soils. J. Soil Mech. Found. Eng. Div. (ASCE) 94(SM4), 981-1001.

[20] Lloret A., Alonso E.E. 1980. Consolidation of unsaturated soils including swelling and collapse. Géotechnique 30(4), 449-477.

[21] Lloret A., Alonso E.E. 1985. State surfaces for partially saturated soils. Dans 11th I.C.S.M.F.E., p. 557-562.

[22] Matyas E.L. 1967. Air and water permeability of compacted soils. Permeability and capillary of soils of compacted soils ASTM STP 417 Amer. Soc. Testing and Materials 2, pp. 160-175.

[23] Mitchell J.K. 1993. Fundamentals of Soil Behavior. W & S Eds. New York. pp 473.

[24] Nützmann G., Maciejewski S., Joswing K. 2002. Estimation of water saturation dependence of dispersion in unsaturated porous media: experiments and modelling analysis.

[25] Philip J.R & De Vries D.A. 1957. Moisture Movement in porous materials under temperature gradents, Trans. Am. Geophys. Un. 38, 222-232

[26] Pfannkuch HO. 1963. Contribution a l'étude des déplacements de fluides miscibles dans un milieu poreux. Revue de l'institut Français du Pétrole. 18, 215-70.

[27] Richards L.A. 1931. Capillary conduction of liquids through porous medium. J. Physics 1, 318-333.

[28] Scheidegger A. E. 1961. General theory of dispersion in porous media, J. Geophys. Res., Vol. 66, pp. 3273-3278.

[29] Schrefler B.A. 1995. F.E. in environmental engineering: coupled thermo-hydro-mechanical processes in porous media including pollutant transport, 7th European autumn school: Non linear modeling of geomaterials with the finite element method, Aussois, France, 1995.

[30] Sultan N. 1997. Etude du comportement thermo-mécanique de l'argile de Boom : Experiences et modélisation. Thèse de doctorat :l'Ecole Nationale des Ponts et Chaussées,310 p.

[31] Thomas H.R., Cleall P.J., Melhuish T.A., Seetharam S.C. 2004. Modelling the thermal-hydraulic-chemical -mechanical (THCM) behavious of bentonite buffers, Proceedings from task force related meeting on buffer and backfill modelling SKB International Progress

report, Sweden, 63-72

[32] Thomas H.R., He Y. 1995. Analysis of coupled heat, moisture and air transfer in a deformable unsaturated soil. Géotechnique, 40(4) :677-689

[33] Van Genuchten MTh, Wierenga PJ. 1976. Mass transfer studies in sorbing porous media. I: Analytical solutions. Soil Sci Soc Am J., 40. 473-80.

[34] Zienkiewicz, O.C., Chan, A.H.C., Pastor, M., Paul, D.K. and Shiomi, T. 1990. Static and dynamic behaviour of soils: a rational approach to quantitative solutions. I. Fully saturated problems. Proc. R. Soc. Land. A 429, 285-309.

[35] Zienkiewicz, O.C., Taylor, R.L., 1989. The finite element method. McGraw-Hill, London.